Quenching of single-particle strengths in direct reactions

J. Manfredi et al.

Phys. Rev. C **104**, 024608 — Published 9 August 2021

DOI: 10.1103/PhysRevC.104.024608

Quenching of single particle strengths in direct reactions

J. Manfredi,[1,2,*] J. Lee,[3] A. M. Rogers,[4] M. B. Tsang,[1,2] W. G. Lynch,[1,2] C. Anderson,[1] J. Barney,[1,2] K. W. Brown,[1,5] B. Brophy,[1] G. Cerizza,[1] Z. Chajecki,[6] G. Chen,[6] J. Elson,[5] J. Estee,[1,2] H. Iwasaki,[1,2] C. Langer,[1,7] Z. Li,[8] C. Loelius,[1,2] C. Y. Niu,[1,8] C. Pruitt,[5] H. Setiawan,[1,2] R. Showalter,[1,2] K. Smith,[9] L. G. Sobotka,[5] S. Sweany,[1,2] S. Tangwancharoen,[1,2] J. R. Winkelbauer,[1,2] Z. Xiao,[10] and Z. Xu[3]

[1]*National Superconducting Cyclotron Laboratory, Michigan State University, East Lansing, MI 48824, USA*
[2]*Department of Physics and Astronomy, Michigan State University, East Lansing, MI 48824, USA*
[3]*Department of Physics, The University of Hong Kong, Pokfulam Road, Hong Kong, China*
[4]*Department of Physics, University of Massachusetts Lowell, Lowell, MA 01854, USA*
[5]*Department of Chemistry, Washington University, St. Louis, MO 63130, USA*
[6]*Department of Physics, Western Michigan University, Kalamazoo, MI 49008, USA*
[7]*FH Aachen University of Applied Sciences, 52066 Aachen, Germany*
[8]*School of Physics and State Key Laboratory of Nuclear Physics and Technology, Peking University, Beijing 100871, China*
[9]*Department of Physics and Astronomy, University of Tennessee, Knoxville, Tennessee 37996, USA*
[10]*Department of Physics, Tsinghua University, Beijing 100084, China*

(Dated: June 1, 2021)

A discrepancy in the asymmetry dependence of spectroscopic factors extracted with different reaction probes calls into question whether the corresponding reaction models are properly understood. In this work, we present extracted spectroscopic factors from the ^{46,34}Ar$(p,d)^{45,33}$Ar transfer reactions in inverse kinematics at a beam energy of 70 MeV/u. The results are consistent with previous measurements of these reactions at a lower beam energy [Lee et al., PRL 104 122701 (2010)], indicating that the transfer reaction is a reliable probe for the nuclear structure of exotic nuclei across a wide energy range. Results from a large body of transfer reaction measurements, (p,pN) measurements, and theoretical nuclear structure studies make a compelling case for much weaker asymmetry dependence than what is observed with single-nucleon knockout reactions on beryllium or carbon targets.

Atomic nuclei consist of interacting fermions. Correlations between individual nucleons modify the single-particle model that assumes nucleons move in a mean-field potential provided by the other nucleons [1, 2]. Short-range correlations arising from strong repulsion at small distances push nucleons to higher momentum single-particle orbitals [1, 3], while long-range correlations between valence nucleons lead to collective behavior [4]. The *spectroscopic factor* (SF) quantifies the occupancy of a given single-particle orbital in a particular nuclear state, and can be studied with cross-section measurements of direct reactions that remove or add single nucleons. Measurements of a variety of nuclear reactions on stable isotopes across a wide mass range show consistent SF reduction to around 60-70% of independent-particle model expectations [5–8]. Although isolated SF measurements can fluctuate with model inputs, previous work has shown that a systematic approach across multiple systems yields consistent results. [7–12].

The study of nuclei far from the valley of stability requires reaction techniques that use inverse kinematics with rare isotope beams, such as single-nucleon transfer, single-nucleon beryllium-induced knockout, and quasifree knockout [8, 13, 14]. There is disagreement among these techniques on the degree of SF quenching as a function of nuclear asymmetry, parametrized by the difference in neutron and proton separation energies ΔS. Intermediate-energy measurements (mostly between 80 and 100 MeV/u) of single-nucleon knockout induced by beryllium or carbon targets indicate that the SFs of the minority nucleons in asymmetric systems are strongly reduced relative to shell-model expectations [8, 15–18]. However, low-energy transfer measurements of exotic species consistently show at most a weak dependence on ΔS [19–22]. Recent quasifree knockout (both $(p,2p)$ and (p,pn)) measurements have provided further evidence for a flat or weak asymmetry dependence [14, 23–25]. Electron scattering measurements on stable nuclei show that short-range correlations more strongly affect minority nucleons [26], but recent theoretical calculations suggest that this manifests in exotic nuclei as a weak asymmetry dependence [27].

The disagreement between transfer and Be/C-induced knockout reactions indicates incomplete theoretical understanding of the reaction mechanisms. This inconsistency is impactful, as each of these methods is used in a wide variety of nuclear physics experiments [28, 29]. Transfer reaction measurements at higher beam energies can serve as a test of consistency of the transfer reaction technique, as well as a bridge to enable direct comparison between results from low-energy transfer and those from Be/C-induced knockout measurements at medium energy. The existing transfer measurements at high energies are only on nuclei near stability [30, 31].

In this article we present reduction factors extracted from the ^{34}Ar(p,d) and ^{46}Ar(p,d) transfer reactions measured at a significantly higher beam energy (70 MeV/u) than in the previous measurement reported in [19].

Agreement on the strength of the asymmetry dependence between this higher-energy measurement and that of Lee et al. [19] would reaffirm the consistency of the transfer method across a wide energy range at high asymmetry. Disagreement between these two measurements would indicate a potential problem with the current understanding of the single-nucleon transfer mechanism for deeply bound nucleons. Another motivation to test the consistency of (p,d) measurements for asymmetric systems at different energies is that the upcoming Facility for Rare Isotope Beams will expand the range of possible transfer reaction measurements, in particular at high beam energy where rates are higher. We present our results, as well as a systematic comparison of asymmetry trends from several experimental and theoretical studies that support a weaker asymmetry dependence than what is observed in Be/C-induced knockout experiments. This discrepancy of the reduction factor remains a key problem in reaction theory that urgently needs to be resolved.

The differential cross sections of the ^{46}Ar$(p,d)^{45}$Ar and ^{34}Ar$(p,d)^{33}$Ar single-neutron transfer reactions at 70 MeV/u were measured at the National Superconducting Cyclotron Laboratory at Michigan State University [32]. Both measurements were kinematically complete, meaning that both the deuteron and the heavy residue were detected. The ^{46}Ar and ^{34}Ar beams were impinged on CH_2 targets of 75 and 25 μm thicknesses, respectively. Outgoing deuterons were detected with the High Resolution Array (HiRA) [33] in coincidence with heavy reaction residues detected in the S800 focal plane [34]. HiRA consisted of 14 charged-particle detector telescopes set up 35 cm from the target with angular coverage between 8 degrees and 40 degrees in the laboratory frame. Each HiRA telescope contained a 65 μm, single-sided, 32-strip ΔE silicon detector, a 1500 μm, double-sided, 32-strip E silicon detector, and an array of four 3.9 cm thick CsI(Tl) scintillator crystals, with each crystal spanning roughly one quadrant of the preceding silicon detectors. The HiRA detectors were calibrated with radioactive sources and energy-loss calculations as described in [35].

Using the energy deposited in the ΔE, E, and CsI(Tl) detectors, deuterons were identified in HiRA using the standard ΔE-E technique. Reaction residues were identified in the S800 focal plane detectors using energy loss and time-of-flight (TOF) information. Two Microchannel Plates (MCPs) designated as MCP0 (1 meter upstream from the target) and MCP1 (10 cm upstream from the target) counted the incoming beam particles. These MCPs also tracked the beam position for each event in order to improve the angular resolution [36].

After gating on the ^{46,34}Ar(p,d) ^{45,33}Ar reaction channels, the excitation energy of the heavy recoil nucleus was reconstructed. Figures 1a and 1b show excitation energy spectra for ^{33}Ar and ^{45}Ar with peaks corresponding to various final states in each argon recoil. We extracted the ground-state-to-ground-state angular distributions by fitting and integrating the ground-state peaks for many angular slices. At forward angles, the standard deviations of the energy spectra are 240 keV for ^{33}Ar and 260 keV for ^{45}Ar. The resolution was slightly worse for the ^{46}Ar beam despite the thinner target because the beam spot was significantly larger than for the ^{34}Ar beam. Separate diagnostic runs with each beam using a thick carbon target indicated negligible background from carbon-induced reactions. The ground-state peak for ^{33}Ar (corresponding to an $l = 0$ transfer) is clearly distinguishable from the first-excited state at $E^* = 1.359$ MeV. In the ^{45}Ar case, we separate contributions from the $f_{7/2}$ ground state ($l = 3$ transfer) and $p_{3/2}$ first-excited state ($l = 1$ transfer, $E^* = 0.542$ MeV) by focusing on forward angles where the cross section of the $l = 1$ transfer is expected to be highest. Figure 1b shows a clear distortion of the ground-state peak due to contribution from the $p_{3/2}$ state. As there are no other states in this energy range in ^{45}Ar, we are able to fit these spectra with a double-Gaussian function where the width of each Gaussian is fixed to 260 keV. The best-fit centroids correspond closely with the expected energies.

The absolute cross-section normalization was determined using MCP1. Figures 1c and 1d show the resulting differential cross-section data in the center-of-mass (COM) frame as well as corresponding Adiabatic Distorted Wave Approximation (ADWA) calculations for the pure single-neutron transfer into the ^{33}Ar ground state and both the ground state and first-excited state of ^{45}Ar. The corresponding data are given in Tables I and II. The lines in each figure show ADWA calculations performed with the TWOFNR code using two separate optical potentials. The first potential is the CH89 global optical model, which is a parametrized fit across data from many different reactions, and uses a conventional Woods-Saxon form for the neutron-bound-state potential [37]. The data for this fit range from 10 to 65 MeV, close to the presently considered beam energy of 70 MeV. The second approach uses the JLM optical model which is microscopically calculated from convoluted nucleon-density distributions for a specific reaction system [38]. In this case, the densities were calculated via a Hartree-Fock (HF) approach using the SkX Skyrme parametrization [39]. We adjust the radius parameter of the bound-state orbital to reproduce the mean-squared radius from the HF calculation as described in [13]. The rms neutron radii for ^{34}Ar and ^{46}Ar were 3.121 fm and 3.559 fm, respectively. This latter cross-section calculation method is referred to below as "JLM+HF".

Consideration of momentum matching is important to ensure the validity of the one-step Distorted Wave Born Approximation used in the ADWA calculations. The product of the momentum transfer q and the radius R at which the transfer reaction occurs should be close (within 1-2 $\hbar$) to the orbital angular-momentum transfer [21]. A beam energy of 70 MeV gives qR of 1.6 and 2.6 for the

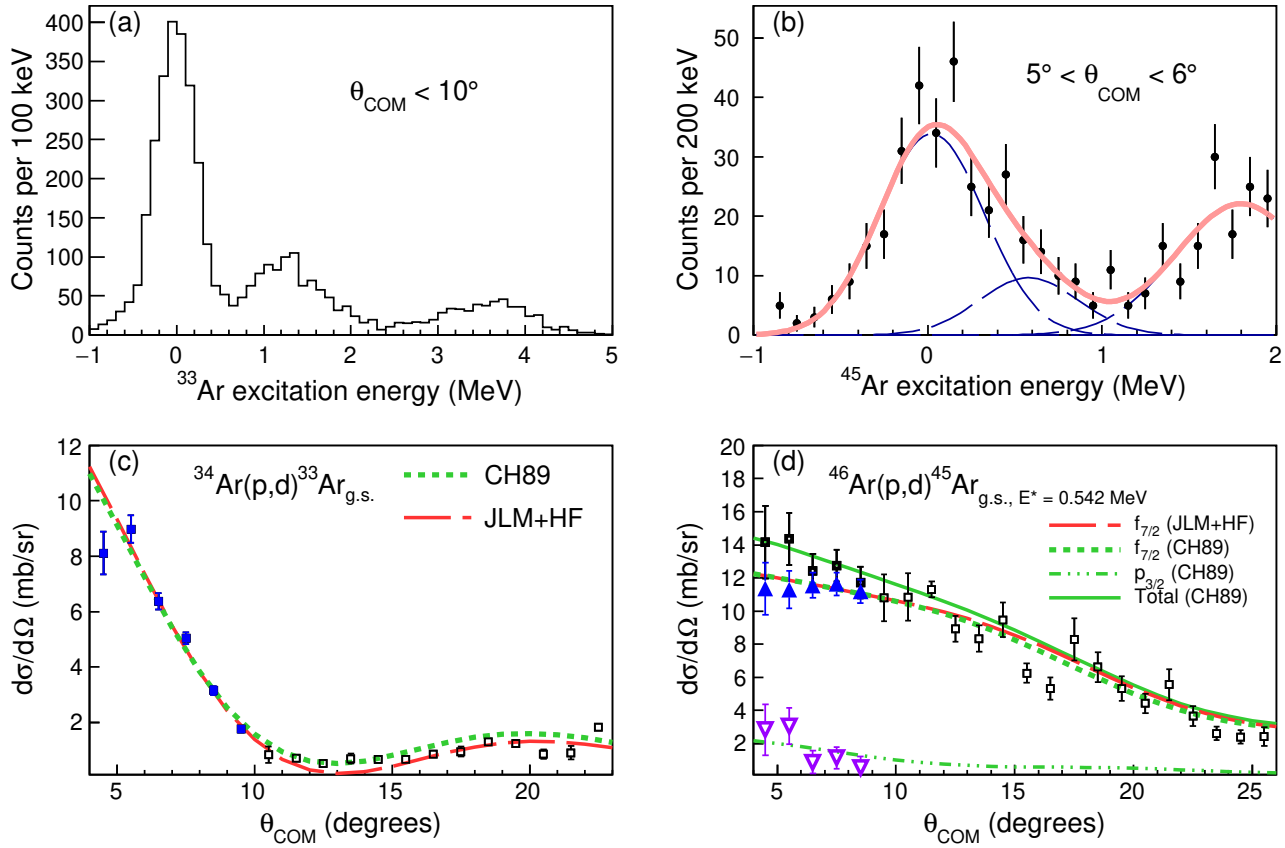

FIG. 1. Example excitation energy spectra for (a) ^{34}Ar$(p,d)^{33}$Ar with a $\theta_{\rm COM}$ (the center-of-mass reaction angle) cut of less than 10 degrees, and (b) ^{46}Ar$(p,d)^{45}$Ar for $\theta_{\rm COM}$ between 5 and 6 degrees. In the latter case, each individual state is modeled using a fixed-width Gaussian (dashed, blue lines), and the total fit is shown by the red, solid line. (c) and (d) show differential cross sections for these two reactions, as well as corresponding ADWA reaction calculations scaled with the SFs to match the data. The blue, solid cross-section points in each plot indicate the data used for SF extraction. In (d), the black, square points correspond to the combined cross section of the ^{45}Ar ground state and first-excited state. At forward angles, contributions from the ground state and first-excited state can be separated (shown as the upward-facing, blue triangles and the downward-facing, purple triangles, respectively).

^{34}Ar(p,d) and ^{46}Ar(p,d) reactions, respectively, and in both cases the values are within reasonable distance of the transferred orbital angular momentum.

Figure 1c shows scaled ADWA calculations for ^{34}Ar$(p,d)^{33}$Ar$_{\rm g.s.}$ using both the CH89 and JLM+HF approaches (the green dotted and red dashed lines, respectively). Figure 1d shows scaled CH89 and JLM+HF calculations for transfer to the ^{45}Ar ground state (again, the green dotted and red dashed lines), and a CH89 calculation for transfer to the first-excited state (green dash-dotted line). There is no JLM+HF cross section calculation for the first-excited state of ^{45}Ar because this requires HF calculations of the nucleon density. Each calculated cross section is scaled with the corresponding extracted SF (as described below).

Given reasonable agreement in the cross-section shape, the experimental SF is the best-fit scaling factor (determined by χ^2 minimization) between the ADWA calculation and the experimental data. Extracted SFs are given in Table III. Uncertainty is calculated by combining in quadrature the 10% uncertainty from the χ^2 minimization with 10% overall normalization uncertainty (determined by studying the stability of the beam normalization over the course of the experiment) to get 14% total uncertainty on each point. For the ^{34}Ar case, we extract the SF from the prominent peak using the six points at the most forward angles (from 4 to 10 degrees in the COM frame). The ^{46}Ar cross section does not have any sharp peaks, and we instead do a χ^2 minimization across the five most forward-angle points (from 4 to 9 degrees in the COM frame) where we can separate the ground-state peak from the low-lying $p_{3/2}$ excited state using the previously described fits. The cross sections to the ground state and first-excited state of ^{45}Ar are shown in Fig. 1d (by the solid, blue triangles and open, purple triangles, respectively) and given in Table II. The sum of

	$d\sigma/d\Omega$ (mb/sr)	
Angle (deg.)	^{34}Ar$(p,d)^{33}$Ar$_{\rm g.s}$	^{46}Ar$(p,d)^{45}$Ar$_{\rm g.s.+}{}_{p_{3/2}}$
4.5	8.11 ± 0.77	14.17 ± 2.20
5.5	8.98 ± 0.49	14.36 ± 1.57
6.5	6.38 ± 0.29	12.42 ± 1.02
7.5	5.03 ± 0.21	12.75 ± 0.95
8.5	3.15 ± 0.16	11.72 ± 0.97
9.5	1.75 ± 0.12	10.79 ± 1.42
10.5	0.82 ± 0.29	10.85 ± 1.42
11.5	0.71 ± 0.08	11.31 ± 0.48
12.5	0.51 ± 0.07	8.94 ± 0.78
13.5	0.69 ± 0.18	8.34 ± 0.80
14.5	0.65 ± 0.07	9.47 ± 1.05
15.5	0.66 ± 0.07	6.25 ± 0.58
16.5	0.86 ± 0.09	5.32 ± 0.68
17.5	0.94 ± 0.17	8.29 ± 1.27
18.5	1.29 ± 0.10	6.61 ± 0.91
19.5	1.23 ± 0.13	5.33 ± 0.75
20.5	0.84 ± 0.17	4.42 ± 0.58
21.5	0.90 ± 0.25	5.55 ± 0.95
22.5		3.64 ± 0.60
23.5		2.60 ± 0.42
24.5		2.39 ± 0.41
25.5		2.41 ± 0.56

TABLE I. Differential cross sections (and associated uncertainties) for ^{34}Ar$(p,d)^{33}$Ar and ^{46}Ar$(p,d)^{45}$Ar into both the ground state and first-excited state in the COM frame.

	$d\sigma/d\Omega$ (mb/sr)	
Angle (deg.)	^{46}Ar$(p,d)^{45}$Ar$_{\rm g.s}$	^{46}Ar$(p,d)^{45}$Ar$_{p_{3/2}}$
4.5	11.35 ± 1.58	2.82 ± 1.53
5.5	11.31 ± 1.13	3.05 ± 1.09
6.5	11.55 ± 0.75	0.87 ± 0.70
7.5	11.63 ± 0.69	1.12 ± 0.65
8.5	11.18 ± 0.71	0.54 ± 0.67

TABLE II. Differential cross sections (and associated uncertainties) for ^{46}Ar$(p,d)^{45}$Ar in the COM frame for both the ground state and first-excited state.

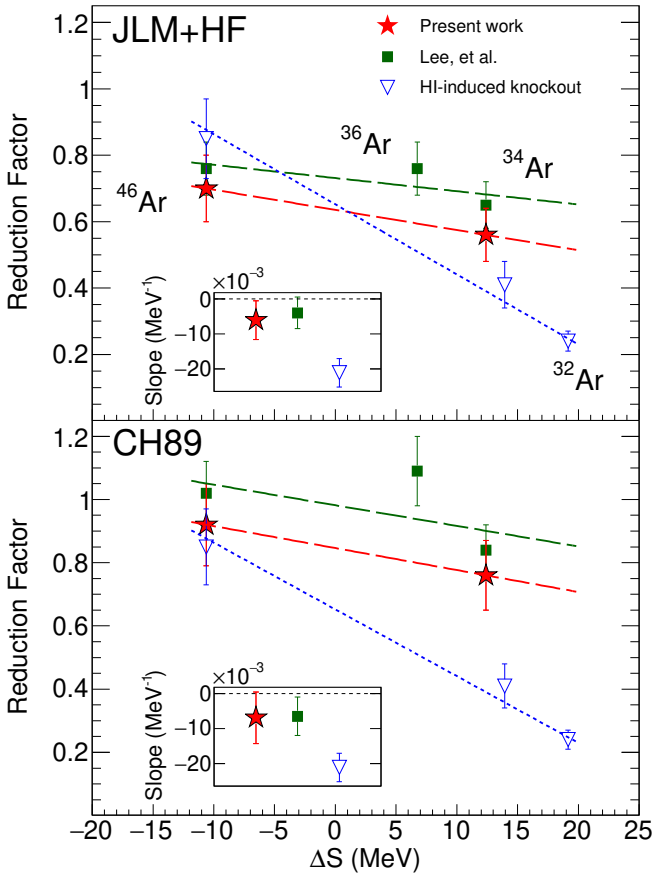

FIG. 2. Asymmetry dependence of reduction factors for 70 MeV/u transfer (the present work, red stars), 33 MeV/u transfer from [19] (green squares), and Be/C-induced knockout (open blue triangles) on argon isotopes [16, 40]. The SFs for the transfer points were extracted using the JLM+HF (top panel) and CH89 (bottom panel) models, as described in the text. The red and green dashed lines correspond to the best linear fits for the 70 MeV/u and 33 MeV/u transfer points, respectively, and the dotted blue line is the best linear fit for the knockout points. The slopes from each fit are shown in the inset plots. The ΔS values for the ^{34}Ar points vary slightly because the knockout measurement was inclusive, as opposed to the exclusive transfer measurements.

these two contributions yields the bold-face, open, black squares. For angles greater than 9 degrees the cross section for both states (black, open squares) is determined by a single Gaussian fit. The sum of the two scaled CH89 calculations is shown by the solid, green line.

The reduction factor for each final state is defined as the ratio of the experimental SF to the large-basis shell model (LBSM) calculation, SF(LBSM). Table III shows the results for the ground-state transfer from ^{34}Ar and ^{46}Ar using both the JLM+HF and CH89 analyses. Figure 2 shows the reduction factors plotted against ΔS for both the JLM+HF (top panel) and CH89 (bottom panel) cases in comparison with low-energy transfer data from [19] and the Be/C-induced knockout data [16, 40] for ^{46}Ar, ^{34}Ar, and ^{32}Ar. Although the magnitude of the individual transfer-reaction reduction factors changes depending on the analysis approach (as discussed in [13]), the slopes of the best-fit linear trends (indicated by the dashed lines) are consistent. The best linear fit for the Be/C-induced knockout data is shown as a blue, dotted line. Inset plots illustrate the slope parameters from each fit: in all transfer-reaction analyses, the slopes with respect to ΔS are less steep than the slope of the Be/C-induced knockout data.

Slopes from reduction-factor data provide a simple and

Isotope	lj^π	ΔS (MeV)	(theo.) SF(LBSM)	(expt.) SF(CH89)	R_s(CH89)	(expt.) SF(JLM+HF)	R_s(JLM+HF)	HF RMS radius (fm)
^{34}Ar	$s^+_{1/2}$	12.40	1.31	1.00 ± 0.14	0.76 ± 0.11	0.73 ± 0.10	0.56 ± 0.08	3.121
^{46}Ar	$f^-_{7/2}$	-10.63	5.16	4.77 ± 0.67	0.92 ± 0.13	3.59 ± 0.50	0.70 ± 0.10	3.559

TABLE III. Extracted spectroscopic factors and reduction factors for both ^{34}Ar and ^{46}Ar.

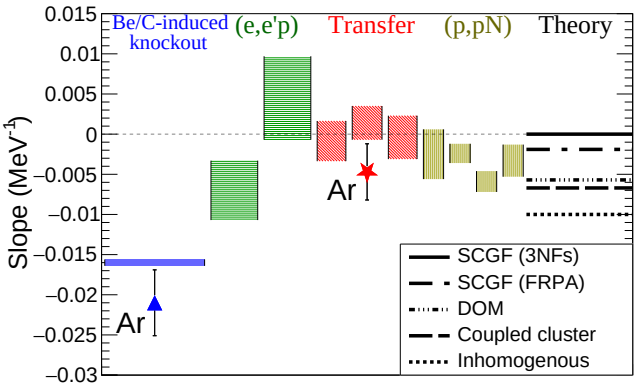

FIG. 3. A summary of reduction-factor slope parameters across different techniques. Details are provided in the text, and the slope values can be found in Table IV with corresponding citations.

model-independent metric for asymmetry dependence for different experimental and theoretical approaches. Figure 3 plots the slope parameters from linear fits of reduction factors and the associated uncertainties (given by the colored bands) for the transfer, Be/C-induced knockout, $(e, e'p)$, and (p, pN) techniques. The blue, Be/C-induced knockout band was calculated via a linear fit of all the data from the seminal compilation by Tostevin and Gade and more recent data from Flavigny, et al. on oxygen isotopes [8, 17]. The blue triangle is from a fit using only argon isotopes [16, 40]. The green, horizontally striped $(e, e'p)$ bands are extracted from two analyses of the NIKHEF measurements, with the results from Kramer, et al. on the left and those from Lapikas, et al. on the right [5, 6]. They are presented with the caveat that both of these studies only include stable isotopes and therefore do not cover a wide asymmetry range. The red, diagonally striped transfer bands represent the ΔS dependence from several transfer-reaction measurements, including a compilation by Xu et al. (leftmost red band) [22] and measurements of oxygen isotopes across a wide asymmetry range by Flavigny et al. (rightmost red band) [20]. The red star corresponds to the slope from a linear fit using transfer-reaction data on argon isotopes only (from both the JLM+HF results presented here and the earlier low-energy measurements [19]). The central transfer band (adjacent to the star) incorporates the present JLM+HF reduction factors with a previous compilation of similarly analyzed data [41, 42]. The gold, vertically striped quasifree knockout bands correspond to separate analyses of data from oxygen, carbon, and nitrogen measurements (both $(p, 2p)$ and (p, pn)). In order from left to right, the bands show results from Phuc et al., Gomez-Ramos et al., Holl et al., and Atar et al. [14, 23–25]. Each of these works employed different theoretical models to extract the SFs, and all exhibit similar asymmetry trends. Together, results from transfer, $(e, e'p)$, and $(p, 2p)$ and (p, pn) experiments indicate a weaker asymmetry dependence than what is observed in knockout reactions using beryllium targets.

The rightmost column of Fig. 3 shows the ΔS dependence of spectroscopic factors obtained from several theoretical calculations, indicated by black lines and labeled in the legend [43–46]. Coupled-cluster calculations from Jensen et al. treat bound states and continuum states on equal footing, and ascribe the observed weak quenching to many-body correlations from neutron scattering states [43]. Self-consistent Green's function (SCGF) results from Barbieri et al. using the Faddeev Random Phase Approximation (FRPA) attempt to account for both short- and long-range correlation effects, and exhibit weak asymmetry dependence [44]. Cipollone et al. also find weak quenching by using the SCGF approach to evaluate the impact of three-nucleon forces on spectroscopic factors [46]. The theoretical model showing the strongest asymmetry dependence calculated radial overlap functions with a nonstandard inhomogenous equation, and calibrated the effective nucleon-nucleon interaction using asymptotic normalization coefficients [45]. Even this approach, however, does not reproduce the magnitude of the quenching seen in the Be/C-induced knockout data.

Slope values for all experimental and theoretical studies are provided in Table IV, as well as the number of data points used for the fit.

Experimental evidence for strong asymmetry dependence has so far only been observed in Be/C-induced knockout reaction data. Considering the large quantity of knockout results on beryllium and carbon targets that consistently show this effect, it is possible that the theoretical knockout model may be incomplete. It could be that the eikonal approximation neglects absorptive processes that uniquely affect deeply bound nucleons [17, 47], the influence of core excitations [48, 49], or a combina-

TABLE IV. Reduction-factor slope parameters for a variety of experimental and theoretical approaches.

Method	References	Slope (MeV^{-1})	Points
Transfer[a]	[42]	0.0014 ± 0.0021	33
Transfer	[22]	-0.00086 ± 0.0025	21
Transfer	[20]	-0.0004 ± 0.0027	7
(p, pN)	[14]	-0.0033 ± 0.0020	5
(p, pN)	[24]	-0.0059 ± 0.0013	15
(p, pN)	[23]	-0.0024 ± 0.0012	14
(p, pN)	[25]	-0.0024 ± 0.0031	18
Knockout (Be/C)	[8, 17]	-0.016 ± 0.00040	34
$(e, e'p)$	[6, 13]	-0.0070 ± 0.0037	10
$(e, e'p)$	[5]	0.0045 ± 0.0052	8
$(e, e'p)$	[51]	-0.012 ± 0.0038	2
SCGF (3NFs) [b]	[46]	-0.000072	15
SCGF (FRPA)[b]	[44]	-0.0019	13
DOM [b]	[52]	-0.0057	11
Coupled-cluster[b]	[43]	-0.0068	10
Inhomogenous[b]	[45]	-0.010	31

[a] Includes the present work
[b] Theoretical nuclear structure calculations

tion of these and other effects. A recent update to the aforementioned Tostevin and Gade compilation of Be/C-induced knockout results shows no significant difference from the original trend, despite including measurements with beam energies up to 1.6 GeV/u [18].

To be complete, however, we note that Atkinson et al. have reanalyzed the NIKHEF data for ^{40}Ca and ^{48}Ca using dispersive optical model (DOM) potentials [50, 51]. The resulting slope is -0.012 ± 0.004 MeV^{-1}, which indicates a stronger dependence than all techniques except for Be/C-induced knockout. We refrain from including this slope in Figure 3 since the two points only cover a small range of asymmetry near stability. Further DOM analysis of other NIKHEF measurements is needed. A previous DOM analysis by Charity at al. that featured 11 calcium isotopes is included in Figure 3 and Table IV.

Recent work on electron scattering data demonstrates that nucleons have a strong preference to form correlated neutron-proton high momentum pairs in the nucleus [26]. To understand how these neutron-proton pairs influence asymmetry dependence, Paschalis et al. explicitly calculated the impact of such short-range correlations (SRC) on the reduction factor as a function of asymmetry using two distinct linear models to account for differences in SRC effects on neutrons and protons [27]. The resulting asymmetry dependence is again weak compared to the quenching seen in the Be/C-induced knockout data.

In conclusion, 70 MeV/u transfer reaction measurements on unstable argon isotopes show much weaker reduction factor asymmetry dependence than what is seen in Be/C-induced knockout results. The available experimental and theoretical evidence generally indicate a weak but non-zero asymmetry dependence, although the error bars from some measurements do overlap with a slope of 0 MeV^{-1}. Agreement between the high-energy transfer measurements shown here and previous low-energy measurements from [19] provides evidence that transfer reactions can be reliably employed to study asymmetric systems at high beam energies for spectroscopic studies when appropriate momentum matching conditions are satisfied [53]. The transfer reaction probe can be further understood via measurements with the high asymmetry beams that will be available at next-generation accelerators like the Facility for Rare Isotope Beams.

The authors would like to thank the operations staff of the NSCL for experimental support. The authors also wish to thank J. Tostevin for use of the TWOFNR program. This work was supported by the National Science Foundation under grant number PHY-1565546. This material is based upon work supported by the U.S. Department of Energy, Office of Science, Office of Nuclear Science, under Award Number DE-FG02-94ER40848 and DE-FG02-87ER-40316. J.M. was supported by a Department of Energy National Nuclear Security Administration Stewardship Science Graduate Fellowship under cooperative Agreement No. DE-NA0002135.

* manfredi@berkeley.edu

[1] W. Dickhoff and C. Barbieri, Progress in Particle and Nuclear Physics **52**, 377 (2004).
[2] L. B. Weinstein, E. Piasetzky, D. W. Higinbotham, J. Gomez, O. Hen, and R. Shneor, Phys. Rev. Lett. **106**, 052301 (2011).
[3] A. Akmal, V. R. Pandharipande, and D. G. Ravenhall, Phys. Rev. C **58**, 1804 (1998).
[4] C. Barbieri, Phys. Rev. Lett. **103**, 202502 (2009).
[5] L. Lapikás, Nuclear Physics A **553**, 297 (1993).
[6] G. Kramer, H. Blok, and L. Lapikás, Nuclear Physics A **679**, 267 (2001).
[7] J. Lee, M. B. Tsang, W. G. Lynch, M. Horoi, and S. C. Su, Phys. Rev. C **79**, 054611 (2009).
[8] J. A. Tostevin and A. Gade, Phys. Rev. C **90**, 057602 (2014).
[9] M. B. Tsang, J. Lee, and W. G. Lynch, Phys. Rev. Lett. **95**, 222501 (2005).
[10] M. B. Tsang, J. Lee, S. C. Su, J. Y. Dai, M. Horoi, H. Liu, W. G. Lynch, and S. Warren, Phys. Rev. Lett. **102**, 062501 (2009).
[11] J. P. Schiffer, C. R. Hoffman, B. P. Kay, J. A. Clark, C. M. Deibel, S. J. Freeman, A. M. Howard, A. J. Mitchell, P. D. Parker, D. K. Sharp, and J. S. Thomas, Phys. Rev. Lett. **108**, 022501 (2012).
[12] F. Flavigny, N. Keeley, A. Gillibert, and A. Obertelli, Phys. Rev. C **97**, 034601 (2018).
[13] J. Lee, J. A. Tostevin, B. A. Brown, F. Delaunay, W. G. Lynch, M. J. Saelim, and M. B. Tsang, Phys. Rev. C **73**, 044608 (2006).
[14] L. Atar, S. Paschalis, C. Barbieri, C. A. Bertulani, P. Díaz Fernández, M. Holl, M. A. Najafi, V. Panin,

H. Alvarez-Pol, T. Aumann, V. Avdeichikov, S. Beceiro-Novo, D. Bemmerer, J. Benlliure, J. M. Boillos, K. Boretzky, M. J. G. Borge, M. Caamaño, C. Caesar, E. Casarejos, W. Catford, J. Cederkall, M. Chartier, L. Chulkov, D. Cortina-Gil, E. Cravo, R. Crespo, I. Dillmann, Z. Elekes, J. Enders, O. Ershova, A. Estrade, F. Farinon, L. M. Fraile, M. Freer, D. Galaviz Redondo, H. Geissel, R. Gernhäuser, P. Golubev, K. Göbel, J. Hagdahl, T. Heftrich, M. Heil, M. Heine, A. Heinz, A. Henriques, A. Hufnagel, A. Ignatov, H. T. Johansson, B. Jonson, J. Kahlbow, N. Kalantar-Nayestanaki, R. Kanungo, A. Kelic-Heil, A. Knyazev, T. Kröll, N. Kurz, M. Labiche, C. Langer, T. Le Bleis, R. Lemmon, S. Lindberg, J. Machado, J. Marganiec-Gałązka, A. Movsesyan, E. Nacher, E. Y. Nikolskii, T. Nilsson, C. Nociforo, A. Perea, M. Petri, S. Pietri, R. Plag, R. Reifarth, G. Ribeiro, C. Rigollet, D. M. Rossi, M. Röder, D. Savran, H. Scheit, H. Simon, O. Sorlin, I. Syndikus, J. T. Taylor, O. Tengblad, R. Thies, Y. Togano, M. Vandebrouck, P. Velho, V. Volkov, A. Wagner, F. Wamers, H. Weick, C. Wheldon, G. L. Wilson, J. S. Winfield, P. Woods, D. Yakorev, M. Zhukov, A. Zilges, and K. Zuber (R^3B Collaboration), Phys. Rev. Lett. **120**, 052501 (2018).

[15] T. Aumann, C. Barbieri, D. Bazin, C. Bertulani, A. Bonaccorso, W. Dickhoff, A. Gade, M. Gómez-Ramos, B. Kay, A. Moro, T. Nakamura, A. Obertelli, K. Ogata, S. Paschalis, and T. Uesaka, Progress in Particle and Nuclear Physics **118**, 103847 (2021).

[16] A. Gade, D. Bazin, B. A. Brown, C. M. Campbell, J. A. Church, D. C. Dinca, J. Enders, T. Glasmacher, P. G. Hansen, Z. Hu, K. W. Kemper, W. F. Mueller, H. Olliver, B. C. Perry, L. A. Riley, B. T. Roeder, B. M. Sherrill, J. R. Terry, J. A. Tostevin, and K. L. Yurkewicz, Phys. Rev. Lett. **93**, 042501 (2004).

[17] F. Flavigny, A. Obertelli, A. Bonaccorso, G. F. Grinyer, C. Louchart, L. Nalpas, and A. Signoracci, Phys. Rev. Lett. **108**, 252501 (2012).

[18] J. A. Tostevin and A. Gade, Phys. Rev. C **103**, 054610 (2021).

[19] J. Lee, M. B. Tsang, D. Bazin, D. Coupland, V. Henzl, D. Henzlova, M. Kilburn, W. G. Lynch, A. M. Rogers, A. Sanetullaev, A. Signoracci, Z. Y. Sun, M. Youngs, K. Y. Chae, R. J. Charity, H. K. Cheung, M. Famiano, S. Hudan, P. O'Malley, W. A. Peters, K. Schmitt, D. Shapira, and L. G. Sobotka, Phys. Rev. Lett. **104**, 112701 (2010).

[20] F. Flavigny, A. Gillibert, L. Nalpas, A. Obertelli, N. Keeley, C. Barbieri, D. Beaumel, S. Boissinot, G. Burgunder, A. Cipollone, A. Corsi, J. Gibelin, S. Giron, J. Guillot, F. Hammache, V. Lapoux, A. Matta, E. C. Pollacco, R. Raabe, M. Rejmund, N. de Séreville, A. Shrivastava, A. Signoracci, and Y. Utsuno, Phys. Rev. Lett. **110**, 122503 (2013).

[21] B. P. Kay, J. P. Schiffer, and S. J. Freeman, Phys. Rev. Lett. **111**, 042502 (2013).

[22] Y. Xu, D. Pang, X. Yun, C. Wen, C. Yuan, and J. Lou, Physics Letters B **790**, 308 (2019).

[23] M. Gómez-Ramos and A. Moro, Physics Letters B **785**, 511 (2018).

[24] M. Holl, V. Panin, H. Alvarez-Pol, L. Atar, T. Aumann, S. Beceiro-Novo, J. Benlliure, C. Bertulani, J. Boillos, K. Boretzky, M. Caamaño, C. Caesar, E. Casarejos, W. Catford, J. Cederkall, L. Chulkov, D. Cortina-Gil, E. Cravo, I. Dillmann, P. D. Fernández, Z. Elekes, J. Enders, L. Fraile, D. G. Redondo, R. Gernhäuser, P. Golubev, T. Heftrich, M. Heil, M. Heine, A. Heinz, A. Henriques, H. Johansson, B. Jonson, N. Kalantar-Nayestanaki, R. Kanungo, A. Kelic-Heil, T. Kröll, N. Kurz, C. Langer, T. L. Bleis, S. Lindberg, J. Machado, E. Nacher, M. Najafi, T. Nilsson, C. Nociforo, S. Paschalis, M. Petri, R. Reifarth, G. Ribeiro, C. Rigollet, D. Rossi, D. Savran, H. Scheit, H. Simon, O. Sorlin, I. Syndikus, O. Tengblad, Y. Togano, M. Vandebrouck, P. Velho, F. Wamers, H. Weick, C. Wheldon, G. Wilson, J. Winfield, P. Woods, M. Zhukov, and K. Zuber, Physics Letters B **795**, 682 (2019).

[25] N. T. T. Phuc, K. Yoshida, and K. Ogata, Phys. Rev. C **100**, 064604 (2019).

[26] O. Hen, M. Sargsian, L. B. Weinstein, and E. Piasetzky, Science **346**, 614 (2014), http://science.sciencemag.org/content/346/6209/614.full.pdf.

[27] S. Paschalis, M. Petri, A. Macchiavelli, O. Hen, and E. Piasetzky, Physics Letters B **800**, 135110 (2020).

[28] K. Wimmer, Journal of Physics G: Nuclear and Particle Physics **45**, 033002 (2018).

[29] P. Hansen and J. Tostevin, Annual Review of Nuclear and Particle Science **53**, 219 (2003), https://doi.org/10.1146/annurev.nucl.53.041002.110406.

[30] P. Alons, J. Kraushaar, and P. Kunz, Physics Letters B **137**, 334 (1984).

[31] R. Anderson, J. Kraushaar, J. Shepard, and J. Comfort, Nuclear Physics A **311**, 93 (1978).

[32] J. Manfredi, *Asymmetry Dependence of Spectroscopic Factors: A Study of Transfer Reactions on Argon Isotopes at 70 MeV/u*, Ph.D. thesis, Michigan State University, East Lansing, MI (2018).

[33] M. Wallace, M. Famiano, M.-J. van Goethem, A. Rogers, W. Lynch, J. Clifford, F. Delaunay, J. Lee, S. Labostov, M. Mocko, L. Morris, A. Moroni, B. Nett, D. Oostdyk, R. Krishnasamy, M. Tsang, R. de Souza, S. Hudan, L. Sobotka, R. Charity, J. Elson, and G. Engel, Nuclear Instruments and Methods in Physics Research Section A: Accelerators, Spectrometers, Detectors and Associated Equipment **583**, 302 (2007).

[34] D. Bazin, J. Caggiano, B. Sherrill, J. Yurkon, and A. Zeller, Nuclear Instruments and Methods in Physics Research Section B: Beam Interactions with Materials and Atoms **204**, 629 (2003), 14th International Conference on Electromagnetic Isotope Separators and Techniques Related to their Applications.

[35] J. Manfredi, J. Lee, W. Lynch, C. Niu, M. Tsang, C. Anderson, J. Barney, K. Brown, Z. Chajecki, K. Chan, G. Chen, J. Estee, Z. Li, C. Pruitt, A. Rogers, A. Sanetullaev, H. Setiawan, R. Showalter, C. Tsang, J. Winkelbauer, Z. Xiao, and Z. Xu, Nuclear Instruments and Methods in Physics Research Section A: Accelerators, Spectrometers, Detectors and Associated Equipment **888**, 177 (2018).

[36] A. Rogers, A. Sanetullaev, W. Lynch, M. Tsang, J. Lee, D. Bazin, D. Coupland, V. Henzl, D. Henzlova, M. Kilburn, M. Wallace, M. Youngs, F. Delaunay, M. Famiano, D. Shapira, K. Jones, K. Schmitt, and Z. Sun, Nuclear Instruments and Methods in Physics Research Section A: Accelerators, Spectrometers, Detectors and Associated Equipment **795**, 325 (2015).

[37] R. Varner, W. Thompson, T. McAbee, E. Ludwig, and T. Clegg, Physics Reports **201**, 57 (1991).

[38] J.-P. Jeukenne, A. Lejeune, and C. Mahaux, Phys. Rev. C **16**, 80 (1977).

[39] B. Alex Brown, Phys. Rev. C **58**, 220 (1998).

[40] A. Gade, P. Adrich, D. Bazin, M. D. Bowen, B. A. Brown, C. M. Campbell, J. M. Cook, T. Glasmacher, P. G. Hansen, K. Hosier, S. McDaniel, D. McGlinchery, A. Obertelli, K. Siwek, L. A. Riley, J. A. Tostevin, and D. Weisshaar, Phys. Rev. C **77**, 044306 (2008).

[41] J. Lee, M. B. Tsang, and W. G. Lynch, Phys. Rev. C **75**, 064320 (2007).

[42] H. Lee, *Survey of Neutron Spectroscopic Factors and Asymmetry Dependence of Neutron Correlations in Transfer Reactions*, Ph.D. thesis, Michigan State University, East Lansing, MI (2010).

[43] O. Jensen, G. Hagen, M. Hjorth-Jensen, B. A. Brown, and A. Gade, Phys. Rev. Lett. **107**, 032501 (2011).

[44] C. Barbieri and W. H. Dickhoff, International Journal of Modern Physics A **24**, 2060 (2009), https://www.worldscientific.com/doi/pdf/10.1142/S0217751X09045625.

[45] N. K. Timofeyuk, Phys. Rev. Lett. **103**, 242501 (2009).

[46] A. Cipollone, C. Barbieri, and P. Navrátil, Phys. Rev. C **92**, 014306 (2015).

[47] R. Shane, R. J. Charity, L. G. Sobotka, D. Bazin, B. A. Brown, A. Gade, G. F. Grinyer, S. McDaniel, A. Ratkiewicz, D. Weisshaar, A. Bonaccorso, and J. A. Tostevin, Phys. Rev. C **85**, 064612 (2012).

[48] C. Louchart, A. Obertelli, A. Boudard, and F. Flavigny, Phys. Rev. C **83**, 011601(R) (2011).

[49] Y. L. Sun, J. Lee, Y. L. Ye, A. Obertelli, Z. H. Li, N. Aoi, H. J. Ong, Y. Ayyad, C. A. Bertulani, J. Chen, A. Corsi, F. Cappuzzello, M. Cavallaro, T. Furono, Y. C. Ge, T. Hashimoto, E. Ideguchi, T. Kawabata, J. L. Lou, Q. T. Li, G. Lorusso, F. Lu, H. N. Liu, S. Nishimura, H. Suzuki, J. Tanaka, M. Tanaka, D. T. Tran, M. B. Tsang, J. Wu, Z. Y. Xu, and T. Yamamoto, Phys. Rev. C **93**, 044607 (2016).

[50] M. C. Atkinson, H. P. Blok, L. Lapikás, R. J. Charity, and W. H. Dickhoff, Phys. Rev. C **98**, 044627 (2018).

[51] M. Atkinson and W. Dickhoff, Physics Letters B **798**, 135027 (2019).

[52] R. J. Charity, L. G. Sobotka, and W. H. Dickhoff, Phys. Rev. Lett. **97**, 162503 (2006).

[53] R. Johnson, E. Stephenson, and J. Tostevin, Nuclear Physics A **505**, 26 (1989).